Enhanced Anomalous Hall Effect of Pt on an Antiferromagnetic Insulator with Fully Compensated Surface

Yu Bai[1,3†], Zhe Wang[3†], Na Lei[6†], Wisal Muhammad[1,3], Lifeng Xiang[1,3], Qiang Li[1,3], Huilin Lai[1,3], Yinyan Zhu[1,2,4], Wenbing Wang[1,2,4], Hangwen Guo[1,2,4], Lifeng Yin[1,2,3,4,5,8*], Ruqian Wu[7*], and Jian Shen[1,2,3,4,5,8*]

[1]*State Key Laboratory of Surface Physics and Institute for Nanoelectronics Devices and Quantum Computing, Fudan University, Shanghai 200433, China*
[2]*Shanghai Qi Zhi Institute, Shanghai 200232, China*
[3]*Department of Physics, Fudan University, Shanghai 200433, China*
[4]*Zhangjiang Fudan International Innovation Center, Fudan University, Shanghai 201210, China*
[5]*Shanghai Research Center for Quantum Sciences, Shanghai 201315, China*
[6]*Fert Beijing Institute, BDBC, School of Electronic and Information Engineering, Beihang University, Beijing 100191, China*
[7]*Department of Physics and Astronomy, University of California, Irvine, California 92697, USA*
[8]*Collaborative Innovation Center of Advanced Microstructures, Nanjing 210093, China*

(Received 1 August 2022; accepted manuscript online 13 September 2022)

We report a significantly enhanced anomalous Hall effect (AHE) of Pt on antiferromagnetic insulator thin film (3-unit-cell $La_{0.7}Sr_{0.3}MnO_3$, abbreviated as LSMO), which is one order of magnitude larger than that of Pt on other ferromagnetic (e.g. $Y_3Fe_5O_{12}$) and antiferromagnetic (e.g. Cr_2O_3) insulator thin films. Our experiments demonstrate that the antiferromagnetic $La_{0.7}Sr_{0.3}MnO_3$ with fully compensated surface suppresses the positive anomalous Hall resistivity induced by the magnetic proximity effect and facilitates the negative anomalous Hall resistivity induced by the spin Hall effect. By changing the substrate's temperature during Pt deposition, we observed that the diffusion of Mn atoms into Pt layer can further enhance the AHE. The anomalous Hall resistivity increases with increasing temperature and persists even well above the Neel temperature (T_N) of LSMO. The Monte Carlo simulations manifest that the unusual rise of anomalous Hall resistivity above T_N originates from the thermal induced magnetization in the antiferromagnetic insulator.

DOI: 10.1088/0256-307X/39/10/108501

The anomalous Hall effect (AHE) often occurs in ferromagnetic materials with either intrinsic [1] or extrinsic [2,3] physical origins, which can be understood within the scope of momentum-space Berry curvatures. [4] Besides the conventional AHE in bulk ferromagnets, interfacial AHE can emerge in nonmagnetic/ferromagnetic metal (FMM) heterostructures due to interfacial scattering. [5–16] To suppress the contribution of bulk AHE from the FMM layer, ferromagnetic insulator (FMI) has been used to replace the conducting FMM layer and an AHE-like transverse contribution due to the spin Hall effect (SHE) was found in a $Pt/Y_3Fe_5O_{12}$ (YIG) heterostructure. [17] Follow-up works have revealed that both the magnetic proximity effect (MPE) and the SHE contribute to AHE of Pt/YIG. [18–22] The MPE induced anomalous Hall effect (MPE-AHE) is pronounced at low temperature, while the SHE induced anomalous Hall effect (SHE-AHE) dominates at elevated temperature. The MPE-AHE and the SHE-AHE have opposite signs and opposite temperature dependences, leading to a sign reversal around 50 K for the anomalous Hall resistance of the Pt/YIG heterostructure, [18,19] as shown in Fig. S1(b) in the Supplementary Information. Similar results have been reported in other systems, such as $Pt/Y_3Fe_{5-x}Al_xO_{12}$, [20] W/YIG, [21] and $Pt/Tm_3Fe_5O_{12}$ (TmIG). [22]

To boost the SHE-AHE and thus the total anomalous Hall resistivity at elevated temperatures, it would be ideal to further suppress the MPE-AHE using antiferromagnetic insulator (AFMI) instead of FMI. Attempts were made using Cr_2O_3 [23] as the AFMI to interface with Pt but no noticeable enhancement of total anomalous Hall resistivity was observed compared to that of the Pt/YIG. [19,20] This is not surprising considering the fact that the surface of the AFMI Cr_2O_3 has an uncompensated spin structure. [24] In this Letter, we use a 3-unit-cell (UC) $La_{0.7}Sr_{0.3}MnO_3$ (LSMO) grown on $SrTiO_3(100)$ substrate, which is known to have a fully compensated surface spin structure, [25–28] as the AFMI layer to interface with Pt. Remarkably, the anomalous Hall resistivity of Pt/3-UC LSMO is enhanced by one order of magnitude compared to that of Pt/YIG because the MPE-AHE is effectively suppressed. The total anomalous Hall resistivity is dominated by SHE-AHE

†Yu Bai, Zhe Wang and Na Lei contributed equally to this work.
*Corresponding authors. Email: lifengyin@fudan.edu.cn; wur@uci.edu; shenj5494@fudan.edu.cn

and increases monotonically with temperature well above the Neel temperature (T_N) of the 3-UC LSMO film. The Monte Carlo simulations indicate that such unusual temperature dependence of the anomalous Hall resistivity originates from the thermo-induced short-range magnetic order in AFMI.

LSMO films were epitaxially grown on $SrTiO_3$ substrates using pulse laser deposition with an energy density of $2\,J/cm^2$ (248 nm, 2 Hz).[25,29] During the growth, the substrate was held at 800 ℃ in an oxygen (8% ozone) environment of 3.5×10^{-3} Torr. The thickness and the growth quality of the films were monitored by reflection high energy electron diffraction (RHEED). After that, the LSMO films were transferred *in situ* into a molecular beam epitaxy chamber with base pressure of 1×10^{-10} Torr for the deposition of 2 nm Pt thin films at room temperature. The Pt/LSMO heterostructures were patterned into the Hall-bar mesa geometry using photolithography and Ar ion beam milling. The sample dimension is shown in Fig. 1(a). The width w of the Hall bar is 100 μm and the distance l between two longitudinal pads is 600 μm. Transport and magnetic measurements were carried out using a Quantum Design physical property measurement system (PPMS) and a superconducting quantum interference device (SQUID), respectively. For transport measurements, the charge current density j_e was applied in the x-direction along the Hall bar, where V_{xx} and V_{xy} are the voltages along the x and y directions, respectively.

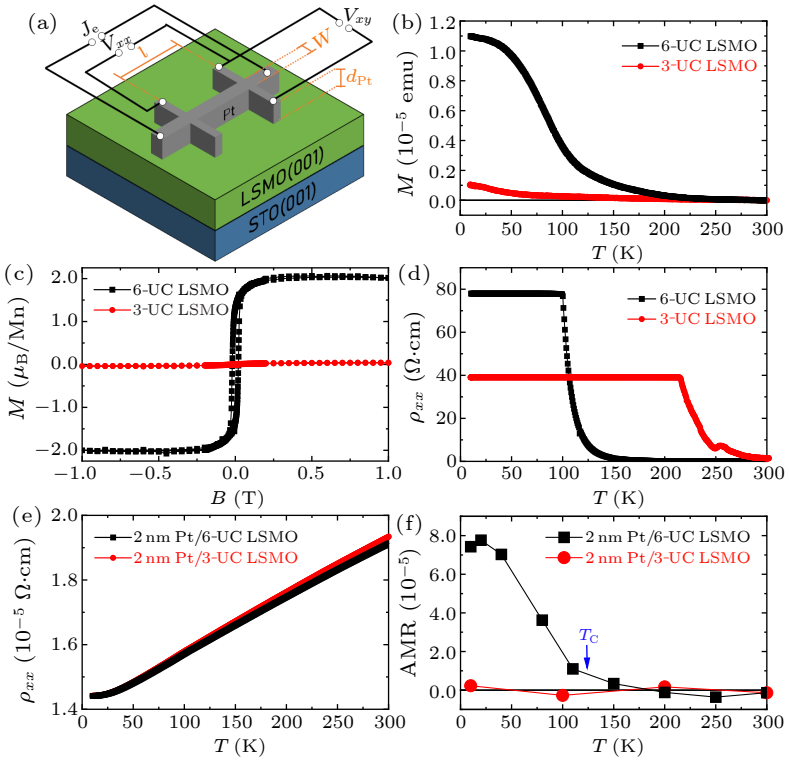

Fig. 1. (a) Schematic of the Pt/LSMO Hall bar samples. (b) M–T curves of LSMO measured by SQUID. (c) Hysteresis loops of 3-UC and 6-UC LSMO samples. (d) ρ–T curves of pure LSMO films measured by PPMS. Both 3-UC and 6-UC LSMOs show insulator behavior. (e) ρ–T curves of Pt/LSMO heterostructure measured by PPMS both show conductor behavior. (f) The temperature dependence of AMR of 2 nm Pt/3-UC LSMO and 2 nm Pt/6-UC LSMO from 10 K to 300 K.

The magnetization versus temperature (M–T) curves of 3-UC and 6-UC LSMO samples (without Pt) are shown in Fig. 1(b) with a 500 Oe magnetic field applied along the surface normal. The M–T curve of the 6-UC LSMO suggests a ferromagnetic behavior with curie temperature (T_C) around 125 K, and the hysteresis loop in Fig. 1(c) gives a saturation magnetic moment of 2 μ_B/Mn. The M–T curve of the 3-UC LSMO only has a small upturn around 40 K, which is consistent with the previous observation of an antiferromagnetic behavior based on exchange bias measurements.[26] The resistivity versus temperature (ρ–T) curves in Fig. 1(d) increase quickly with cooling, and even beyond the limit of Keithley 2400 source meter at low temperature, which indicates that both samples are well defined insulators. In comparison, the resistivity of the 2 nm Pt capped LSMO films [Fig. 1(e)] drops by 7 orders of magnitude, which ensures that the electric current flows within the Pt layer. Figure 1(f) shows the result of anisotropic magneto resistance (AMR) measurement with 1.5 T magnetic field, calculated by $\Delta\rho_{xx}/\rho_{xx}$. According to the AMR results, there is no MPE in the case of Pt/3-UC LSMO, while MPE does exist in Pt/6-UC LSMO below T_C (125 K).

The field-dependent Hall resistivity can be calculated

by $\rho_{xy} = (V_{xy}/I_{xx})d_{\rm Pt}$, where $d_{\rm Pt}$ is the thickness of the Pt layer; ρ_{xy} includes the ordinary Hall resistivity ($\rho_{\rm OHE}$) and the anomalous Hall resistivity ($\rho_{\rm AHE}$) and can be expressed as $\rho_{xy} = \rho_{\rm OHE} + \rho_{\rm AHE}$. After subtracting $\rho_{\rm OHE}$, we plot magnetic-field-dependent $\rho_{\rm AHE}$ of the Pt/3-UC LSMO measured at various temperatures from 10 K to 375 K in Fig. 2(a). It is clear that the sign of $\rho_{\rm AHE}$ remains negative in this temperature range, unlike the sign reversal of Pt/YIG at 50 K.[18] Since the MPE in Pt/3-UC LSMO is absent based on our AMR measurements in Fig. 1(f), we may conclude that the measured $\rho_{\rm AHE}$ mainly results from the SHE-AHE. In fact, $\rho_{\rm AHE}$ has negative sign even at 10 K, which is rescaled in Fig. 2(c) for a better view.

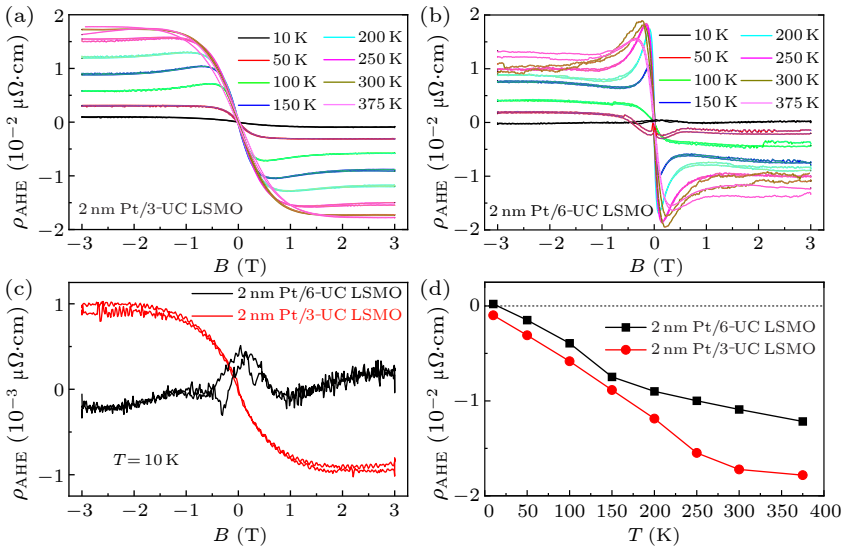

Fig. 2. (a) and (b) Magnetic field dependence of $\rho_{\rm AHE}$, obtained from 10 K to 375 K with the magnetic field along z direction from −3 T to 3 T of 2 nm Pt on 3-UC LSMO and 6-UC LSMO. (c) The field dependence of $\rho_{\rm AHE}$ of 2 nm Pt/3-UC LSMO and 2 nm Pt/6-UC LSMO at 10 K, which clearly show the sign reversal. (d) The temperature dependence of $\rho_{\rm AHE}$ of 2 nm Pt/3-UC LSMO and 2 nm Pt/6-UC LSMO from 10 K to 375 K.

Strikingly, as shown in Fig. 2(a), $\rho_{\rm AHE}$ of the Pt/3-UC LSMO increases with temperature even above $T_{\rm N}$, and finally saturates around 375 K. While such kind of temperature dependence is opposite to that of Pt/YIG,[30] similar behavior was also observed in Pt/Cr_2O_3,[23] implying that the interfacial AHE in Pt/AFMI may have a different physical origin. This is especially true considering the fact that the net magnetization of AFMI becomes vanishingly small above $T_{\rm N}$ as in the case of the present 3-UC LSMO system. For the 6-UC LSMO, although the global physical behavior is similar to that of an FMI, it has a more complicated magnetic configuration than the pure FMI state in YIG. According to our previous studies for 6-UC LSMO,[25] the bottom 3-UC LSMO is in the pure AFMI phase, while the topmost 3-UC is phase separated FMM domains inside an AFMI matrix. As shown in Fig. 2(c), the positive sign of $\rho_{\rm AHE}$ and the none zero coercivity field at 10 K clearly indicate the existence of MPE in Pt/6-UC LSMO, similar to that of Pt/YIG below 50 K.[18] The $\rho_{\rm AHE}$ at 50 K in Fig. 2(b) displays a butterfly-like behavior as a result of the competition between the SHE-AHE and the MPE-AHE. Further increasing temperature to 100 K (near $T_{\rm c}$), the MPE is vanishingly small and the total AHE is dominated by the SHE-AHE with a negative sign. Beyond 150 K, the $\rho_{\rm AHE}$ curves show a pronounced upturn at the saturation field, which appears to originate from the topological Hall effect (THE) due to the thermally driven spin chirality fluctuation near the domain boundary of the AFM phase and the FM phase in the 6-UC LSMO. Similar THE has also been observed in Pt on systems with complex magnetic configurations above their ordering temperature, such as Pt/TmIG[31] and Pt/Cr_2O_3.[23]

Figure 2(d) shows the saturated $\rho_{\rm AHE}$ deduced from Figs. 2(a) and 2(b) under a magnetic field of 3 T as a function of temperature for Pt on the 3-UC and 6-UC LSMO films. With the increase of temperature, the magnitude of $\rho_{\rm AHE}$ of the Pt/3-UC LSMO sample increases from 1.0×10^{-3} μΩ·cm at 10 K to 1.8×10^{-2} μΩ·cm at 375 K, which is one order of magnitude larger than that of the Pt/YIG.[19,20] For the Pt/6-UC LSMO sample, $\rho_{\rm AHE}$ changes from about 2.1×10^{-4} μΩ·cm at 10 K to -1.2×10^{-2} μΩ·cm at 375 K with a sign reversal. To show the enhancement, the Hall resistance and anomalous Hall resistance of Pt/YIG and Pt/LSMO are compared side by side in Fig. S1 in the Supplementary Information.

To better understand the nature of the interfacial AHE in the Pt/LSMO system, we carried out several controlled experiments. Figures 3(a) and 3(b) show the $\rho_{\rm AHE}$ versus temperature for Pt grown at 75 K, 300 K and 370 K on the 3-UC and the 6-UC LSMO films, respectively. In general, higher growth temperature of Pt tends to generate more intermixing between Mn and Pt, which should affect the SHE-AHE accordingly. For both cases, $\rho_{\rm AHE}$ is larger when Pt is grown at higher temperature. For example, $\rho_{\rm AHE}$ of Pt deposited at 370 K is one order of magnitude larger than that of Pt deposited at 75 K for the measur-

ing temperature of 375 K. This evidently indicates that the SHE-AHE is enhanced by the intermixing between Mn and Pt atoms. Figure 3(c) shows the Pt thickness dependence of $\rho_{\rm AHE}$ for Pt grown on the 3-UC LSMO. The $\rho_{\rm AHE}$ value decreases with increasing Pt thickness, confirming that the interfacial effect plays the key role. Indeed, insertion of a 2 nm Cu layer between Pt and 6-UC LSMO completely diminishes the AHE, with only ordinary Hall effect left as shown in Fig. 3(d). For comparison, the Hall resistivity ρ_{xy} of 2 nm Pt/6-UC LSMO without the subtraction of $\rho_{\rm OHE}$ is also shown in Fig. 3(d), which exhibits the same linear slope. Results of these controlled experiments all prove that the AHE in the present Pt/LSMO systems originates from the interface of Pt/LSMO. To investigate the role of Mn impurities in Pt, we measured the Hall resistivity of 2 nm $Pt_{100}Mn_1/SrTiO_3(001)$. As shown in Fig. S2(a) in the Supplementary Information, AHE is almost unvisitable, which proves that only the diluted Mn impurities in Pt at the interface are not sufficient to exhibit AHE, and it needs the help of underlying LSMO through the exchange interaction.

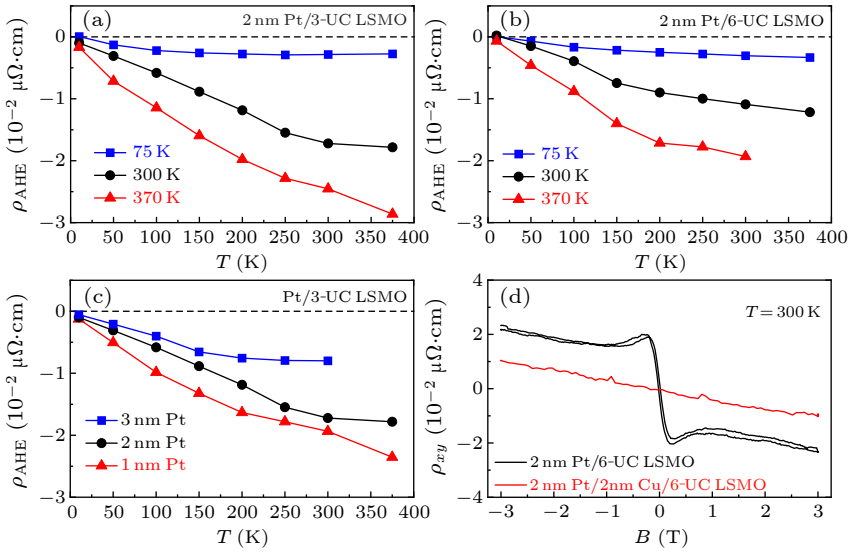

Fig. 3. (a) and (b) Temperature dependence of $\rho_{\rm AHE}$ for 2 nm Pt/3-UC LSMO and 2 nm Pt/6-UC LSMO grown at substrate temperatures of 75 K, 300 K, and 370 K, respectively. (c) Temperature dependence of $\rho_{\rm AHE}$ of 1 nm, 2 nm and 3 nm Pt on 3-UC LSMO grown at 300 K. (d) Magnetic field dependence of ρ_{xy} (without the subtraction of $\rho_{\rm OHE}$) of 2 nm Pt/6-UC LSMO and 2 nm Pt/2 nm Cu/6-UC LSMO deposited and measured at 300 K.

Another puzzle is the origin of AHE above $T_{\rm N}$ in our system. For finite size AFM systems such as nanoparticles, it has been reported that thermal fluctuation can induce a net magnetization.[32] The two spin sublattices in AFM nanoparticles exhibit asymmetric moment canting under an external magnetic field, resulting in a nonzero magnetization as sketched in Fig. 4(a). Thermal fluctuation in fact turns to increase the canting asymmetries and produces net moment in AFM systems. Such a thermal induced magnetization is shown to increase linearly with temperature. As a matter of fact, the existence short-range magnetic order in AFM manganites has been observed at temperatures as high as 530 K, which is 4.5 times higher than their $T_{\rm N}$.[33] To further prove this argument, we measured the Hall resistivity of 2 nm Pt/2 nm $Mn/SrTiO_3(001)$. As shown in Fig. S2(b) in the Supplementary Information, although $T_{\rm N}$ of bulk Mn is 95 K, AHE clearly appears at 100 K and gets significantly enhanced at 300 K, which is the evidence of the existence of short-range magnetic order above $T_{\rm N}$.

For the same reason, nonzero magnetization can be induced by the thermal fluctuation in the AFM LSMO layer in our samples. Such a thermal induced magnetization may modulate the AHE through two mechanisms. Firstly, the spin current reflection at the interface is enhanced, resulting in stronger SHE-AHE with increasing temperature. Secondly, there are diffused Mn atoms in the Pt layers near the interface region. The magnetic moments of these Mn impurities can be pinned through the exchange interaction with the underlying LSMO, producing extra berry-phase contribution toward the anomalous Hall resistivity. To demonstrate this, we performed systematic Monte Carlo (MC) simulations.

Our MC simulations are based on a classical Heisenberg model described by the following Hamiltonian:

$$H = -\frac{1}{2}\sum_{ij} J_{ij} S_i \cdot S_j - K\sum_i (S_i^z)^2 + g\mu_{\rm B} B \cdot S_i^z,$$

where $J_{\rm ij}$ represents exchange interactions, K is the single-ion magnetic anisotropy, $g = 2$ is the electron spin g factor, $\mu_{\rm B}$ is the Bohr magneton, and B is the external magnetic field. The model of Pt/LSMO interface is shown in Fig. 4(b), which contains 3-UC AFM LSMO and one layer of Mn impurities. Each layer of LSMO has 30×30 spins represented by a unit vector S_i, and the Mn impurity layer consists of evenly distributed 10×10 spins. To capture the C-AFM nature of the LSMO layer, its inter-layer exchange interaction was set to the corresponding bulk

value, $J_\perp = 22.5\,\text{meV}$ (FM), while the intra-layer exchange interaction was set to $J_\parallel = -10\,\text{meV}$ (AFM). The exchange interaction J_{int} between Mn in Pt and Mn in LSMO was assumed to be 20 meV. For the single-ion magnetic anisotropy of Mn in LSMO, we adopted a typical value of $K = 0.1\,\text{meV}$. An external magnetic field of $B = 3\,\text{T}$ was applied to lift the degeneracy. We used 10^4 MC steps per site to equilibrate the system, and 10^5 MC steps per site for statistical averaging.

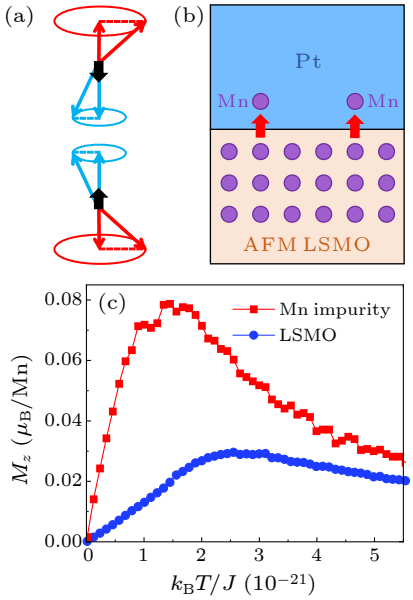

Fig. 4. (a) Schematic illustration of the two uniform precession modes exited by thermal fluctuations in AFM materials. The red and blue arrows are magnetization vectors of the sublattices, and the black arrow is the net magnetization. The two modes are degenerated without external magnetic fields. (b) Schematic model of our Monte Carlo simulations. (c) Magnetization of Mn in LSMO and Mn impurities in Pt as a function of temperature.

The simulated magnetization as a function of temperature is shown in Fig. 4(c), in which the blue and red lines represent net magnetic moments of Mn in LSMO and Mn in Pt, respectively. At zero temperature, the magnetic moments of both LSMO layer and Mn impurities are zero. When the temperature increases, a finite magnetization emerges and increases with temperature up to T_N. This thermally induced magnetic moment decreases very slowly above T_N, which may explain why the AHE of Pt/Cr_2O_3 [23] and Pt/LSMO survive well above ordering temperature. Through the exchange interaction between Mn atoms across the interface, Mn-impurities embedded in Pt show larger magnetic moments, about 2.7 times higher compared to the largest magnetic moment of Mn atoms in the AFM LSMO layer. Obviously, the interdiffusion of Mn is another important factor that enhances the AHE of Pt/LSMO as observed in our experiments.

In summary, a 3-UC LSMO/STO (100) thin film with fully compensated surface allows the observation of a pure SHE-AHE when interfaced with Pt. In addition, the diffusion of Mn atoms into the Pt layers near the interface can further enhance the SHE-AHE. These two effects make the anomalous Hall resistivity of Pt/3-UC LSMO one order of magnitude larger than that of Pt/YIG. Interestingly, the anomalous Hall resistivity increases with increasing temperature even beyond T_N. Based on our Monte Carlo simulation, the temperature dependence is attributed to thermally induced magnetization in AFMI LSMO and adjacent Mn atoms. The significantly enhanced AHE at interfaces of heavy metal and AFMI above room temperature is highly valuable for applications of antiferromagnetic spintronics. [34]

Acknowledgments. This work was supported by the National Key Research Program of China (Grant No. 2020YFA0309100), the National Natural Science Foundation of China (Grant Nos. 11991062, 12074075, 12074073, 12074071, and 11904052), the Shanghai Municipal Science and Technology Major Project (Grant No. 2019SHZDZX01), and the Shanghai Municipal Natural Science Foundation (Grant Nos. 20501130600, 22ZR1407400, and 22ZR1408100).

References

[1] Karplus R and Luttinger J M 1954 *Phys. Rev.* **95** 1154
[2] Smit J 1958 *Physica* **24** 39
[3] Berger L 1970 *Phys. Rev. B* **2** 4559
[4] Nagaosa N, Sinova J, Onoda S, MacDonald A H, and Ong N P 2010 *Rev. Mod. Phys.* **82** 1539
[5] Vavra W, Lee C H, Lamelas F J, He H, Clarke R, and Uher C 1990 *Phys. Rev. B* **42** 4889
[6] Keskin V, Schmalhorst B A J, Reiss G, Zhang H, Weischenberg J, and Mokrousov Y 2013 *Appl. Phys. Lett.* **102** 022416
[7] Shaya O, Karpovski M, and Gerber A 2007 *J. Appl. Phys.* **102** 043910
[8] Rosenblatt D, Karpovski M, and Gerber A 2010 *Appl. Phys. Lett.* **96** 022512
[9] Guo Z B, Mi W B, Aboljadayel R O, Zhang B, Zhang Q, Barba P G, Manchon A, and Zhang X X 2012 *Phys. Rev. B* **86** 104433
[10] Kou X L, Schmalhorst J M, Keskin V, and Reiss G 2012 *J. Appl. Phys.* **112** 093915
[11] Tsui F, Chen B X, Barlett D, Clarke R, and Uher C 1994 *Phys. Rev. Lett.* **72** 740
[12] Canedy C L, Li X W, and Xiao G 1997 *J. Appl. Phys.* **81** 5367
[13] Christides C and Speliotis T 2005 *J. Appl. Phys.* **97** 013901
[14] Moritz J, Rodmacq B, Auffret S, and Dieny B 2008 *J. Phys. D* **41** 135001
[15] Zhao J, Wang Y J, Han X F, Zhang S, and Ma X H 2010 *Phys. Rev. B* **81** 172404
[16] Xu W J, Zhang B, Liu Z X, Wang Z, Li W, Wu Z B, Yu R H, and Zhang X X 2010 *Europhys. Lett.* **90** 27004
[17] Nakayama H, Althammer M, Chen Y T, Uchida K, Kajiwara Y, Kikuchi D, Ohtani T, Geprägs S, Opel M, Takahashi S, Gross R, Bauer G E W, Goennenwein S T B, and Saitoh E 2013 *Phys. Rev. Lett.* **110** 206601
[18] Huang S Y, Fan X, Qu D, Chen Y P, Wang W G, Wu J, Chen T Y, Xiao J Q, and Chien C L 2012 *Phys. Rev. Lett.* **109** 107204
[19] Zhou X, Ma L, Shi Z, Fan W J, Zheng J G, Evans R F L, and Zhou S M 2015 *Phys. Rev. B* **92** 060402(R)

[20] Liang X, Shi G Y, Deng L J, Huang F, Qin J, Tang T T, Wang C T, Peng B, Song C, and Bi L 2018 *Phys. Rev. Appl.* **10** 024051

[21] Ma L, Fu H R, Tang M, Qiu X P, Shi Z, You C Y, Tian N, and Zheng J G 2020 *Appl. Phys. Lett.* **117** 122405

[22] Ding S L, Liang Z Y, Yun C, Wu R, Xue M Z, Lin Z C, Ross A, Becker S, Yang W Y, Ma X B, Chen D F, Sun K, Jakob G, Kläui M, and Yang J B 2021 *Phys. Rev. B* **104** 224410

[23] Cheng Y, Yu S S, Zhu M L, Hwang J, and Yang F Y 2019 *Phys. Rev. Lett.* **123** 237206

[24] Wu N, He X, Wysocki A L, Lanke U, Komesu T, Belashchenko K D, Binek C, and Dowben P A 2011 *Phys. Rev. Lett.* **106** 087202

[25] Chen H Y, Yu Y, Wang Z, Bai Y, Lin H X, Li X L, Liu H, Miao T, Kou Y F, Zhang Y S, Li Y, Tang J, Wang Z C, Cai P, Zhu Y Y, Cheng Z H, Zhong X Y, Wang W B, Gao X Y, Yin L F, Wu R Q, and Shen J 2019 *Phys. Rev. B* **99** 214419

[26] Shi Y J, Zhou Y, Ding H F, Zhang F M, Pi L, Zhang Y H, and Wu D 2012 *Appl. Phys. Lett.* **101** 122409

[27] Lepetit M B, Mercey B, and Simon C 2012 *Phys. Rev. Lett.* **108** 087202

[28] Tebano A, Aruta C, Sanna S, Medaglia P G, Balestrino G, Sidorenko A A, De Renzi R, Ghiringhelli G, Braicovich L, Bisogni V, and Brookes N B 2008 *Phys. Rev. Lett.* **100** 137401

[29] Shen J, Ward T Z, and Yin L F 2013 *Chin. Phys. B* **22** 017501

[30] Uchida K I, Qiu Z Y, Kikkawa T, Iguchi R, and Saitoh E 2015 *Appl. Phys. Lett.* **106** 052405

[31] Ahmed A S, Lee A J, Bagués N, McCullian B A, Thabt A M A, Perrine A, Wu P, Rowland J R, Randeria M, Hammel P C, McComb D W, and Yang F Y 2019 *Nano Lett.* **19** 5683

[32] Mørup S and Frandsen C 2004 *Phys. Rev. Lett.* **92** 217201

[33] Hermsmeier B, Osterwalder J, Friedman D J, and Fadley C S 1989 *Phys. Rev. Lett.* **62** 478

[34] Baltz V, Manchon A, Tsoi M, Moriyama T, Ono T, and Tserkovnyak Y 2018 *Rev. Mod. Phys.* **90** 015005

Supplementary Information for
Enhanced Anomalous Hall Effect of Pt on an Antiferromagnetic Insulator with Fully Compensated Surface

Yu Bai *et al.*

Lifeng Yin, Ruqian Wu, Jian Shen
Email: lifengyin@fudan.edu.cn, wur@uci.edu, shenj5494@fudan.edu.cn

The field dependence and the temperature dependence of Hall resistance R_H and anomalous Hall resistance R_{AHE} of Pt/YIG and Pt/LSMO are compared side by side in Fig. S1. The sign reversal around 50 K for the anomalous Hall resistance R_{AHE} of the 10 nm Pt/YIG heterostructure is clearly seen in Fig. S1 (b), while R_{AHE} of the 2 nm Pt/3UC LSMO remains negative at all measured temperatures in Fig. S1 (d). The R_{AHE} value of the 10 nm Pt/YIG at 300 K is one order of magnitude smaller than the ordinary Hall resistance R_{OHE}. Without the subtraction of R_{OHE}, the contribution of R_{AHE} at 300 K is almost invisible in Fig. S1 (a). In stark contrast, the R_{AHE} value of the 2 nm Pt/3UC LSMO at 300K is almost 3 times larger than the R_{OHE} value as shown in Fig. S1 (c) and (d).

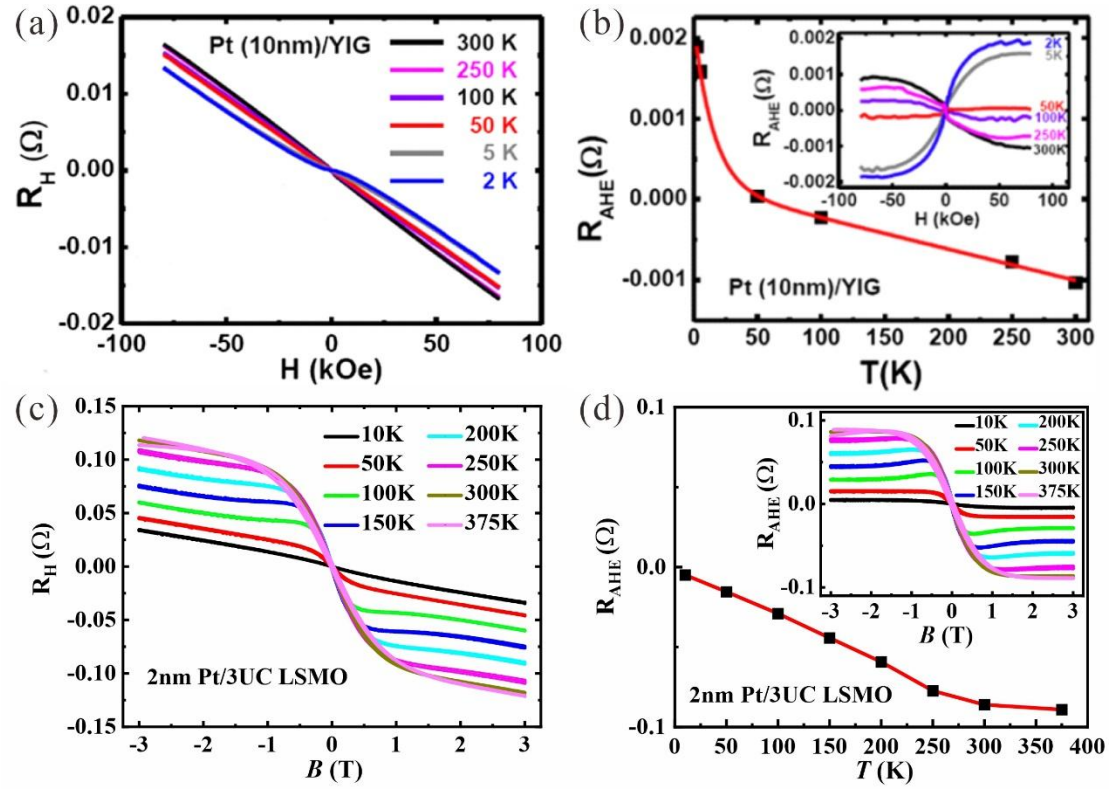

Fig. S1 (a) Field dependence of Hall resistance R_H at different temperatures for 10 nm Pt/YIG (copied from Ref. [1]). (b) The anomalous Hall resistance R_{AHE} as a function of the temperature for 10 nm Pt/YIG (copied from Ref. [1]). The inset shows R_{AHE} as a function of magnetic field. (c) Field dependence of R_H at different temperatures for

2 nm Pt/3UC LSMO. (d) R_{AHE} as a function of the temperature for 2 nm Pt/3UC LSMO. The inset shows R_{AHE} as a function of magnetic field.

The diffusion of Mn into the Pt at the Pt/LSMO interface is important, but the diffusion of Mn itself can't yield sizable AHE. As reported by Ning An *et al.* [2], the $Mn_{1-x}Pt_x$ epitaxial films can show large AHE, but only at the composition of Mn_3Pt, which is known as a noncollinear antiferromagnet in $L1_2$ structure. It is deposited under the optimized sputtering power of Mn target to make sure the right Mn_3Pt stoichiometry and annealed at 600 ℃ to make sure the right $L1_2$ structure. These critical conditions don't fit in our case, where the Mn impurities in the Pt are diluted. To know the role of the interdiffusion of Mn, we measured the Hall resistivity of 2 nm $Pt_{100}Mn_1/SrTiO_3(001)$. As shown in the Fig. S2 (a), AHE is almost unvisitable. It proves that only the diluted Mn impurities in Pt at the interface are not sufficient to exhibit AHE, and it needs the help of underlying LSMO through the exchange interaction.

In addition, we have measured the Hall resistivity of 2 nm Pt/2 nm $Mn/SrTiO_3(001)$. As shown in the Fig. S2 (b), although T_N of bulk Mn is 95 K, AHE clearly appears at 100K and gets significantly enhanced at 300 K. Since both Mn and Pt layers are conducting, the contribution of AHE from Mn layer and Pt layer are mixed. However, by comparing the magnitude of ρ_{AHE} of 2 nm Pt/2 nm Mn sample (1.5×10^{-1} μΩ·cm) and 2nm Pt/3 UC LSMO sample (1.8×10^{-2} μΩ·cm) at 300K, we can conclude AHE is mainly from the Mn layer due to the short-range order above T_N.

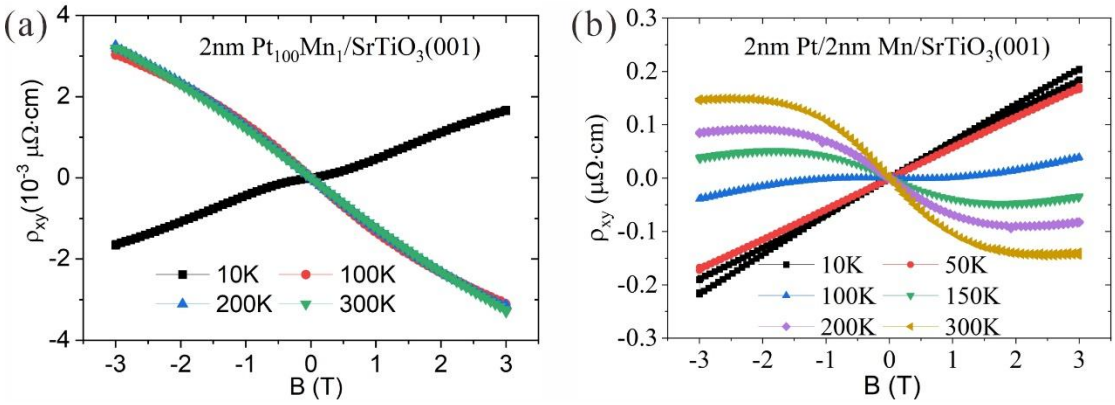

Fig. S2 (a) Field dependence of Hall resistivity at different temperatures for 2 nm $Pt_{100}Mn_1/SrTiO_3(001)$. (b) Field dependence of Hall resistivity at different temperatures for 2 nm Pt/2 nm $Mn/SrTiO_3(001)$.

Reference

[1] S.Y. Huang, X. Fan, D. Qu, Y.P. Chen, W.G. Wang, J. Wu, T.Y. Chen, J. Q. Xiao, and C.L. Chien, Physical Review Letters 109, 107204 (2012).

[2] N. An, M. Tang, S. Hu, H.L. Yang, W.J. Fan, S.M. Zhou, and X.P. Qiu, Sci. China-Phys. Mech. Astron. 63, 297511 (2020).